International Journal of Greenhouse Gas Control 21 (2014) 91–100

Contents lists available at ScienceDirect

International Journal of Greenhouse Gas Control

journal homepage: www.elsevier.com/locate/ijggc

Process analysis of intensified absorber for post-combustion CO_2 capture through modelling and simulation

Atuman S. Joel, Meihong Wang*, Colin Ramshaw, Eni Oko

Process/Energy Systems Engineering Group, School of Engineering, University of Hull, HU6 7RX, UK

ARTICLE INFO

Article history:
Received 29 May 2013
Received in revised form
10 November 2013
Accepted 2 December 2013
Available online 27 December 2013

Keywords:
Post-combustion
CO_2 capture
Chemical absorption
Process intensification (PI)
Rotating packed bed (RPB)
Process simulation

ABSTRACT

Process intensification (PI) has the potential to significantly reduce capital and operating costs in post-combustion CO_2 capture using monoethanolamine (MEA) solvent for power plants. The intensified absorber using rotating packed bed (RPB) was modelled based on Aspen Plus® rate-based model, but some build-in correlations in Aspen Plus® rate-based model were replaced with new correlations suitable for RPB. These correlations reflect centrifugal acceleration which is present in RPB. The new correlations were implemented in visual FORTRAN as sub-routines and were dynamically linked to Aspen Plus® rate based model. The model for intensified absorber was validated using experimental data and showed good agreement. Process analysis carried out indicates: (a) CO_2 capture level increases with rotating speed. (b) Higher lean MEA inlet temperature leads to higher CO_2 capture level. (c) Increase in lean MEA concentration results in increase in CO_2 capture level. (d) Temperature bulge is not present in intensified absorber. Compared with conventional absorber using packed columns, the insights obtained from this study are (1) intensified absorber using RPB improves mass transfer significantly. (2) Higher flue gas temperature or lean MEA temperature will not be detrimental to the reactive separation as such cooling duty for flue gas can be saved. (3) Inter-cooling cost will not be incurred since there is no temperature bulge. A detail comparison between conventional absorber and intensified absorber using RPB was carried out and absorber volume reduction factor of 12 times was found. These insights can be useful for design and operation of intensified absorber for CO_2 capture.

1. Introduction

Greenhouse gas (GHG) emissions have become a concern for the global community in the 21st century. This is because of the rapid increase in population and corresponding increase in energy demand. Combustion of coal and petroleum accounts for the majority of CO_2 emissions. Petroleum is mostly used as a transportation fuel for vehicles while coal is used mostly for electricity generation, for instance about 85.5% of coal is used for electricity generation in 2011 in the UK (DECC, 2012). Coal-fired power plants are therefore the largest stationary source of CO_2.

Intergovernmental panel on climate change (IPCC) has set ambitious goal to reduce CO_2 emission by 50% in 2050 as compared to the level of 1990. CO_2 capture technology is important for meeting the target. Post-combustion CO_2 capture with chemical absorption is the most matured CO_2 capture technology. As such, it is considered a low-risk technology and a promising near-term option for large-scale CO_2 capture (MacDowell et al., 2010).

Post-combustion CO_2 Capture for coal-fired power plants using conventional absorber has been reported by many authors. Lawal et al. (2009a,b, 2010) carried out dynamic modelling of CO_2 absorption for post-combustion capture in coal-fired power plants. Dugas (2006) carried out experimental study of post-combustion CO_2 capture in the context of fossil fuel-fired power plants. In these studies, one of the identified challenges to the commercial roll out of the technology has been the large size of the packed columns needed. This translates to high capital and operating cost and unavoidable impact on electricity cost. Approaches such as heat integration, inter-cooling among others could reduce the operating cost slightly. However, they limit the plant flexibility and will make operation and control more difficult (Kvamsdal et al., 2009). PI has the potential to meet this challenge (Reay, 2008).

1.1. Motivation

BERR (2006) reported that a 500 MWe supercritical coal fired power plant operating at 46% efficiency (LHV basis) releases over 8000 tonnes of CO_2 per day. Post-combustion CO_2 capture from the flue gas based on the conventional technology will require very large packed columns. Dynamic modelling study of a 500 MWe subcritical coal-fired power plant by Lawal et al. (2012) showed that

* Corresponding author. Tel.: +44 01482 466688; fax: +44 01482 466664.
E-mail addresses: Meihong.Wang@hull.ac.uk, wang_2003_uk@yahoo.co.uk (M. Wang).

1750-5836
http://dx.doi.org/10.1016/j.ijggc.2013.12.005

Nomenclature

A	gas–liquid interfacial area (m^2/m^3)
a_t	total specific surface area of packing (m^2/m^3)
D_L	diffusivity coefficient of liquid (m^2/s)
d_p	diameter of packing pore (m)
g_c	gravitational acceleration or acceleration due to centrifugal field (m^2/s)
g_o	characteristic acceleration value ($100\ m^2/s$)
k_L	liquid phase mass transfer coefficient (m/s)
L	superficial mass velocity of liquid ($kg/m^2\ s$)
Q_L	volumetric flow rate of liquid (m^3/s)
R	radial position (m)
T	temperature (K)
U	superficial flow velocity (m/s)
U_o	characteristic superficial flow velocity (1 cm/s)
$y_{CO_2,\,in}$	mole fraction of CO_2 in inlet stream
$y_{CO_2,\,out}$	mole fraction of CO_2 in outlet stream
Z	axial height of the packing (m)

Greek letters

ε	porosity of packing
ε_L	liquid holdup
μ	viscosity (Pa s)
ρ_L	liquid density (kg/m^3)
ρ_G	gas density (kg/m^3)
σ	liquid surface tension (N/m)
σ_c	critical surface tension (N/m)
ν_L	kinematic liquid viscosity (m^2/s)
ω	angular velocity (rad/s)

Dimensionless groups

Fr_L	Froude number ($L^2 a_t/g_c$)
Gr_L	liquid Grashof number ($d_p^2 g_c/\nu_L^2$)
Re_L	liquid Reynolds number ($L/a_t\nu_L$)
Sc_L	liquid Schmidt number (ν_L/D_L)
We_L	liquid Webber number ($L^2\rho_L/a_t\sigma$)

two absorbers of 17 m in packing height and 9 m in diameter will be needed to separate CO_2 from the flue gas. These huge conventional packed columns will mean higher capital and operating costs. This could increase electricity costs by over 50% and has been a major impediment to commercializing the technology. On the other hand, PI has potentials of significant cost reduction. As a result, detailed study of PI application in post-combustion CO_2 capture is necessary.

1.2. Use of process intensification (PI) for CO_2 capture

PI technology was invented in the late 1970s and early 1980s. RPB, a typical PI equipment, was invented by Ramshaw and Mallinson (1981) for enhancing the gas–liquid mass transfer in distillation and absorption processes. The technology promotes size and weight reduction, enhances inherent safety with lower inventories, improves energy consumption, lower capital cost, and addresses environmental concerns (Jassim et al., 2007). With RPB, intensification is achieved by rotation of the equipment during operation. The associated centrifugal acceleration leads to droplet flow and film flow of liquids in the unit. This will increase interfacial area and consequently mass transfer. Based on this, vessel size will therefore be reduced significantly compared to conventional absorbers (Jassim et al., 2007; Wang et al., 2011; Cheng and Tan, 2011).

Trevor (1998) reported that one of the ways to get friendliness in plant design can be achieved by the use of intensification. He defined friendliness in a plant as the existence of low inventory of hazardous materials such that it may not matter if the entire inventory leaks.

The absorber rig using RPB is shown in Fig. 1. Flue gas is passed through the stainless steel shaft to the packed bed and it is contacted counter-currently with lean-MEA solution. MEA chemically absorbs CO_2 in the flue gas leaving the treated gas with lower CO_2 content. The treated gas is vented into the environment. The rich MEA solution stream is sent to a stripper for regeneration of the lean MEA solution.

1.3. Estimating height and diameter of packed bed as related to RPB absorber

Fig. 2 explains how the geometry of the intensified absorber using RPB can be related to conventional packed column for our study.

Packing height of intensified absorber using RPB in this paper is estimated as the difference between the outer and inner radius of RPB.

$$\text{packing height}\,(H) = r_o - r_i \tag{1}$$

The diameter of the intensified absorber using RPB is calculated from volume relation.

$$V_{RPB} = V_{CPB} \tag{2}$$

1.4. Novel contributions of the paper

There are three novel aspects in this paper: (a) model development of intensified absorber using RPB. This involved modifying the rate-based absorber model in Aspen Plus® to capture the behaviour of a RPB absorber by replacing the default correlations with new ones suitable for RPB. The new correlations written in visual FORTRAN are dynamically linked with the Aspen Plus® rate-based model. The model presented in this paper is equivalent as developing a new model for RPB case even though it is still in Aspen Plus®. Related modification is reported by Prada et al. (2012). However, their modifications were for distillation rather than packed column for CO_2 absorption. (b) Model validation. Model predictions were compared to the experimental data given by Jassim et al. (2007). It indicates good agreement. (c) With the model developed and validated, process analysis of the RPB absorber was carried out to gain insights for process design and operation. It was found that cooling duty for flue gas can be greatly reduced since for RPB absorber higher temperature contributes to increase in CO_2 capture level. Temperature bulge problem in RPB absorber is not there since it is being operated at low residence time as such costs associated with inter-cooling will be saved. Comparison between conventional absorber using packed column and intensified absorber using RPB shows a reduction factor of 12 times.

2. Model development

Modelling and simulation of conventional packed column for post-combustion CO_2 capture has been reported in Freguia and Rochelle (2003), Kvamsdal and Rochelle (2008) and Lawal et al. (2009a,b, 2010). In this paper, the RPB absorber was modelled in Aspen Plus® using the rate-based absorber model from the Aspen Plus® model library with its default correlations replaced by new correlations suitable for intensified absorber using RPB. These new correlations reflect centrifugal acceleration which is present in RPB. The new correlations were implemented in visual FORTRAN as sub-routines. The sub-routines were dynamically linked to Aspen Plus® rate based model. These correlations include some equations presented in Tung and Mah (1985) and Onda et al. (1968)

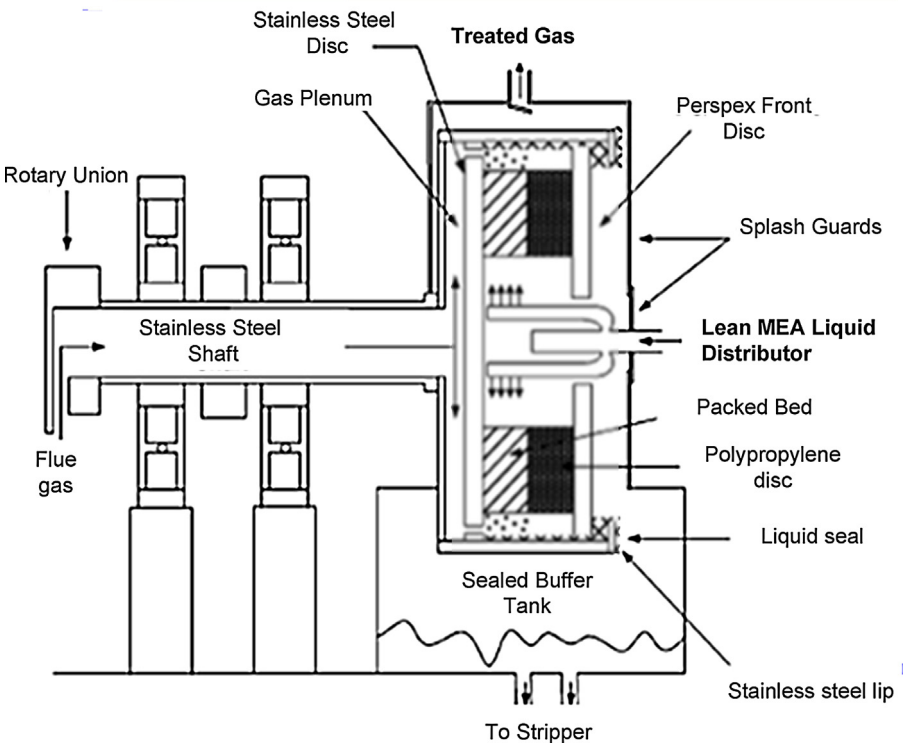

Fig. 1. Cross-sectional view of the HIGEE rig (Jassim et al., 2007).

for liquid and gas phase mass transfer coefficient respectively. Tung and Mah (1985) correlation is modified to reflect centrifugal acceleration present in RPB. ONDA correlation, modified by updating the gravity term in the equation with centrifugal acceleration, is used to estimate interfacial area. Liquid holdup is evaluated using Burns et al. (2000) equation. Dry pressure drop expression which accounts in an additive manner of the drag and centrifugal forces, the gas–solid slip and radial acceleration effect given by Llerena-Chavez and Larachi (2009) was used. Electrolyte Non-Random-Two-Liquid (ElecNRTL) activity coefficient model is used for physical properties calculation. The coefficient of equilibrium constant and equilibrium reactions which are assumed to occur in the liquid film are found in Biliyok et al. (2012). Kinetic reaction equations and parameters are obtained in AspenTech (2010). Process parameters can be found in Jassim et al. (2007). In this study, VPLUG flow model option is applied meaning that the outlet conditions at each segment are used for the bulk of liquid phase and the average conditions are used for the bulk of the vapour phase (Kvamsdal and Rochelle, 2008).

2.1. Liquid phase mass transfer coefficient

An expression was introduced by Tung and Mah (1985) using the penetration model to describe the liquid mass transfer behaviour in the RPB.

$$\frac{k_L d_p}{D_L} = 0.919\left(\frac{a_t}{a}\right)^{1/3} Sc_L^{1/2} Re_L^{2/3} Gr_L^{1/6} \quad (3)$$

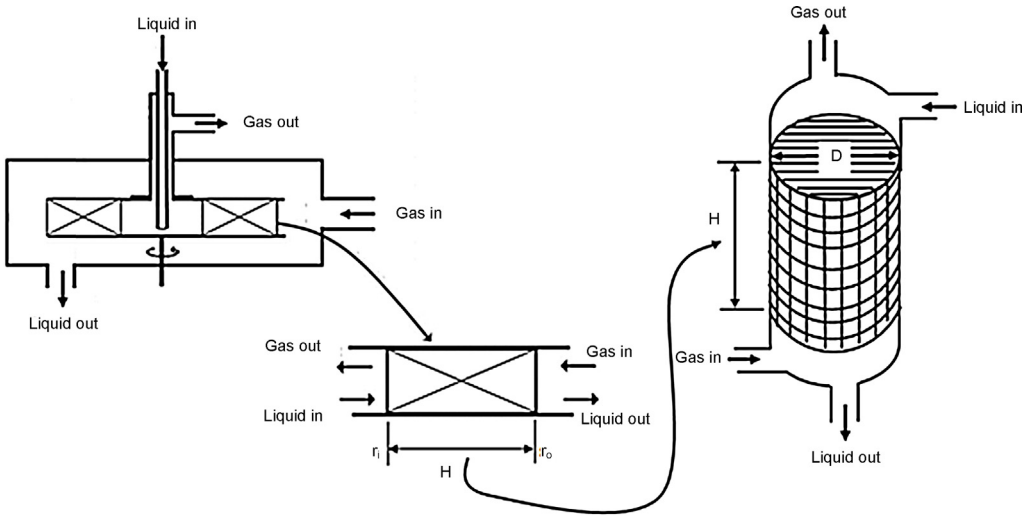

Fig. 2. Relating volume of RPB to conventional packed bed.

g_c in the Grashof number is taken as $g_c = rw^2$ to account for the effect of rotation in the RPB absorber.

2.2. Total gas–liquid interfacial area

Total gas–liquid interfacial area is calculated with the Onda et al. (1968) correlation.

$$\frac{a}{a_t} = 1 - \exp\left[-1.45\left(\frac{\sigma_c}{\sigma}\right)^{0.75} Re_L^{0.1} We_L^{0.2} Fr_L^{-0.05}\right] \quad (4)$$

Similarly, g_c in the Froude number is taken as $g_c = rw^2$ to account for the effect of rotation in the RPB absorber.

2.3. Liquid hold-up

Liquid holdup correlation by Burns et al. (2000) is given as:

$$\varepsilon_L = 0.039\left(\frac{g_c}{g_o}\right)^{-0.5}\left(\frac{U}{U_o}\right)^{0.6}\left(\frac{\nu}{\nu_o}\right)^{0.22}$$
$$g_o = 100\,\text{m s}^{-2}, \quad U_o = 1\,\text{cm s}^{-1}, \quad \nu_o = 1\,\text{cS} = 10^{-6}\,\text{m}^2\,\text{s}^{-1} \quad (5)$$

$$U = \frac{Q_L}{2\pi r Z} \quad (6)$$

2.4. Dry pressure drop expression

Semi-empirical dry pressure drop expression is given by Llerena-Chavez and Larachi (2009) as:

$$\Delta P_{\text{Packed bed}} = \frac{150(1-\varepsilon)^2\mu}{d^2\varepsilon^3}\left(\frac{G}{2\pi Z}\right)\ln\frac{r_o}{r_i} + \frac{1.75(1-\varepsilon)\rho}{d\varepsilon^3} \times \left(\frac{G}{2\pi Z}\right)^2\left(\frac{1}{r_i} - \frac{1}{r_o}\right) + \frac{1}{2}\rho\omega^2(r_o^2 - r_i^2) + F_c \quad (7)$$

where F_c is a corrective function given as:

$F_c = \varepsilon(a - G + (b + \omega^c)G^2)$

a, b, and c are fitting parameters given as:

$a = -0.08\,\text{m}^3/\text{s} \quad b = 2000\,(\text{rpm})^c \quad c = 1.22$

2.5. Modelling and simulation methodology

The procedure used in this paper for modelling and simulation of the RPB is shown in Fig. 3.

3. Model validation

The experimental data used for model validation was obtained from Jassim (2002) and Jassim et al. (2007). From their experiments, two lean-MEA concentration (average 55 wt% and 75 wt%) were selected so as to fall within a reasonable range of MEA concentration to minimize the problem of corrosion and maximize CO_2 absorption rate. Two different lean-MEA flow rates were selected, one having the lean-MEA flow rate of 0.66 kg/s and the other having lean-MEA flow rate of 0.35 kg/s. This is to achieve different liquid to gas (L/G) mass ratios. Four cases were considered.

Case 1: Lean-MEA flow rate of 0.66 kg/s and average MEA concentration of 55 wt%. Case 2: Lean-MEA flow rate of 0.35 kg/s and average MEA concentration of 55 wt%. Case 3: Lean-MEA flow rate of 0.66 kg/s and average MEA concentration of 75 wt%. Case 4: Lean-MEA flow rate of 0.35 kg/s and average MEA concentration of 75 wt%.

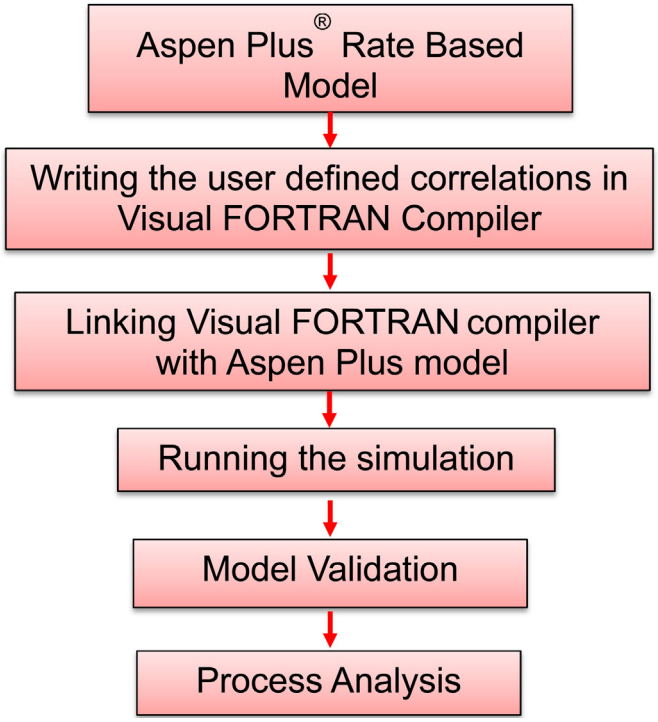

Fig. 3. Methodology used in this paper.

Each of the four cases has four runs. The runs differ from each other by either lean-MEA temperature or rotor speed. Two different rotor speeds (600 rpm and 1000 rpm) were used.

Table 1 gives the input process conditions for Case 1 and Case 2 having average MEA concentration of 55 wt% while Table 2 gives the input process conditions for Case 3 and Case 4 having average MEA concentration of 75 wt%.

RPB absorber packing is modelled with 7 RateFrac segments. Same simulation for 12 RateFrac segments were performed for same packing height and it was found that capture level difference was less than 1%. Based on that, all the validation studies were done with 7 RateFrac segments.

Using volume relationship described in Section 1.3, the packing height of our RPB model is 0.121 m and the diameter is 0.166 m. The packing type used is coil with void fraction of 0.76 and surface area of 2132 m^2/m^3.

Validation results were presented in terms of CO_2 capture level and CO_2 penetration which are defined in Eqs. (8) and (9) respectively.

$$CO_2 \text{ capture level } (\%) = \left(\frac{y_{CO_2,\text{in}} - y_{CO_2,\text{out}}}{y_{CO_2,\text{in}}}\right) \times 100 \quad (8)$$

$$CO_2 \text{ penetration } (\%) = (1 - CO_2 \text{ capture level}) \quad (9)$$

In Table 3, the model predictions were compared to experimental data at the input conditions shown in Table 1. In all the runs considered for Cases 1 and 2, relative error of prediction for almost all the various variables assessed is less than 7% except in Case 1 Run 2 where the error prediction on CO_2 capture level is 11.0964%.

In Table 4, the simulation predictions were compared to experimental data at the input conditions shown in Table 2. The results for Case 3 and Case 4 show that for all runs the error prediction is less than 8% except Case 3 Run 2 where the error prediction on CO_2 capture level is 11.8883%.

The results show that the model developed using Aspen Plus® rate-based absorber model modified with new correlations suitable for RPB absorber is able to reasonably capture the behaviour

Table 1
Input process conditions at MEA concentration range of 53–57 wt% (Jassim, 2002).

Variable	Case 1				Case 2			
	Run 1	Run 2	Run 3	Run 4	Run 5	Run 6	Run 7	Run 8
Rotor speed (RPM)	600	600	1000	1000	600	600	1000	1000
Lean temperature (°C)	39.6	20.7	40.1	20.9	39.5	22.3	39.6	22.6
Lean pressure (atm.)	1	1	1	1	1	1	1	1
Flue gas flow rate (kmol/h)	2.87	2.87	2.87	2.87	2.87	2.87	2.87	2.87
CO_2 composition in flue gas (vol%)	4.71	4.60	4.48	4.45	4.43	4.47	4.35	4.09
Lean-MEA flow rate (kg/s)	0.66	0.66	0.66	0.66	0.35	0.35	0.35	0.35
Lean-MEA composition (wt%)								
H_2O	40.91	43.35	40.91	42.40	41.01	40.11	41.03	39.10
CO_2	3.09	3.45	3.09	3.60	3.99	3.89	3.97	3.90
MEA	56.00	53.20	56.00	54.00	55.00	56.00	55.00	57.00

Table 2
Input process conditions at MEA concentration range of 72–78 wt% (Jassim, 2002).

Variable	Case 3				Case 4			
	Run 1	Run 2	Run 3	Run 4	Run 5	Run 6	Run 7	Run 8
Rotor speed (RPM)	600	600	1000	1000	600	600	1000	1000
Lean temperature (°C)	41	21.4	40.2	20.7	40.8	22.1	39.4	20.6
Lean pressure (atm.)	1	1	1	1	1	1	1	1
Flue gas flow rate (kmol/h)	2.87	2.87	2.87	2.87	2.87	2.87	2.87	2.87
CO_2 composition in flue gas (vol%)	4.40	4.36	4.36	4.29	3.55	4.38	4.38	4.53
Lean-MEA flow rate (kg/s)	0.66	0.66	0.66	0.66	0.35	0.35	0.35	0.35
Lean-MEA composition (wt%)								
H_2O	22.32	20.83	23.41	23.00	24.95	21.57	22.16	19.71
CO_2	2.68	2.17	2.59	1.90	3.05	2.43	2.84	2.29
MEA	75.00	77.00	74.00	75.10	72.00	76.00	75.00	78.00

of an intensified absorber using RPB. This is because Jassim et al. (2007) reported that the CO_2 measurement in the gas sample has a reproducibility of ±0.6% and in the liquid sample CO_2 and MEA measurement has reproducibility of ±1.6% and ±1.4% respectively. Also error created as result of rotation can increase the CO_2 capture level error. Error reported in Tables 3 and 4, of less than 12% is reasonably good. As a result, the model can be used to analyze typical RPB behaviour at different input conditions.

4. Process analysis

In this section, the model developed and validated is used to analyze the process characteristics of the intensified absorber using RPB.

4.1. Effect of rotor speed on CO_2 capture level

4.1.1. Justification for case study

Energy requirement for an RPB depends on the rotor speed which in turn affects the capture level. As a result, it is important to understand the relationship that rotor speed bears with capture level so that the energy requirement for maintaining the speed can be maximized with respect to capture level.

4.1.2. Setup of the case study

To do this, the rotor speed was varied from 400 rpm to 1200 rpm. This range was chosen to cover the validated rotor speeds of 600 rpm and 1000 rpm in Section 3. Two lean-MEA temperatures, 20.9 °C and 39.5 °C, were chosen. This is needed to study the impact of the rotor speed at lower and higher temperature conditions. Again, two MEA concentrations were chosen to explore the impact of varying rotor speed on CO_2 capture level.

The case study setup input conditions are shown in Case1 Run 1 of Table 1 for 56 wt% MEA concentration and Case 3 Run 1 of Table 2 for 75 wt% MEA concentration. In both cases, rotor speed changes as 400 rpm, 600 rpm, 800 rpm, 1000 rpm and 1200 rpm.

4.1.3. Results and discussions

Figs. 4 and 5 show effects of varying rotor speed on CO_2 capture level for 56 wt% and 75 wt% lean MEA concentrations at 20.9 °C and 39.5 °C lean MEA temperatures. The results show that CO_2 capture level increases with increase in rotor speed for both 20.9 °C and 39.5 °C lean MEA temperatures due to enhanced mass transfer. Rotation of the absorber enhances mass transfer by stimulating combined droplet and film flow (Burns et al., 2000). This behaviour increases with rotor speed. Also, at higher rotor speed the problem of liquid mal-distribution is overcome leading to higher wetted area which subsequently contributes to improving mass transfer.

Figs. 4 and 5 also show that CO_2 capture levels at different rotor speed are affected by the lean MEA temperatures. At 20.9 °C lean MEA temperature, CO_2 capture level increases more significantly

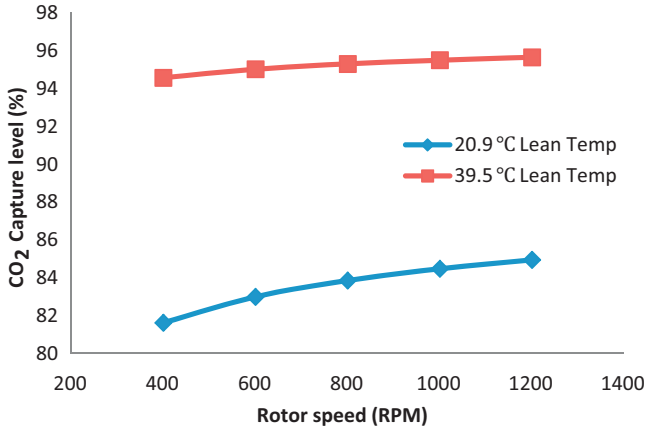

Fig. 4. Effect of rotor speed on CO_2 capture level at 56 wt% MEA.

Table 3
Simulation results compared to the experimental data for Case 1 and Case 2.

Variable7 c	Case 1											
	Run 1			Run 2			Run 3			Run 4		
	Expt.	Model	Relative error (%)	Expt.	Model	Relative error (%)	Expt.	Model	Relative error (%)	Expt.	Model	Relative error (%)
CO_2 loading of lean MEA, (mol CO_2/mol MEA)	0.0772	0.0772		0.0897	0.0897		0.0772	0.0772		0.0924	0.0924	
CO_2 loading of rich MEA, (mol CO_2/mol MEA)	0.0822	0.0830	1.0949	0.0951	0.0956	0.5257	0.0822	0.0828	0.8516	0.0955	0.0980	2.6178
Average lean MEA/rich MEA, (mol CO_2/mol MEA)	0.0797	0.0801	0.6273	0.0924	0.0926	0.2165	0.0797	0.0800	0.3764	0.0940	0.0952	1.2766
CO_2 capture level (%)	94.9	93.56	0.8746	83	92.21	11.0964	95.4	94.06	1.4046	87.0	92.79	6.6552
CO_2 penetration (%)	5.1	6.44		17	7.79		4.6	5.94		13.0	7.21	
Variable	Case 2											
	Run 5			Run 6			Run 7			Run 8		
	Expt.	Model	Relative error (%)	Expt.	Model	Relative error (%)	Expt.	Model	Relative error (%)	Expt.	Model	Relative error (%)
CO_2 loading of lean MEA, (mol CO_2/mol MEA)	0.1000	0.1000		0.0955	0.0955		0.0996	0.0996		0.0945	0.0945	
CO_2 loading of rich MEA, (mol CO_2/mol MEA)	0.1105	0.1106	0.0905	0.1044	0.1054	0.9579	0.1073	0.1096	2.1435	0.1021	0.1034	1.2733
Average lean MEA/Rich MEA, (mol CO_2/mol MEA)	0.1053	0.1056	0.2849	0.1000	0.1005	0.5000	0.1035	0.1047	1.1594	0.0983	0.0989	0.6104
CO_2 capture level (%)	87	90.03	3.4828	84.1	88.58	5.3270	89.9	90.78	0.9789	86.2	89.33	3.6311
CO_2 penetration (%)	13	9.97		15.9	11.42		10.1	9.22		13.8	10.67	

Table 4
Simulation results compared to the experimental data for Case 3 and Case 4.

Variable	Case 3											
	Run 1			Run 2			Run 3			Run 4		
	Expt.	Model	Relative error (%)	Expt.	Model	Relative error (%)	Expt.	Model	Relative error (%)	Expt.	Model	Relative error (%)
CO_2 loading of lean-MEA, (mol CO_2/mol MEA)	0.0492	0.0492		0.0389	0.0389		0.0483	0.0483		0.0355	0.0355	
CO_2 loading of rich-MEA, (mol CO_2/mol MEA)	0.0531	0.0533	0.3766	0.0420	0.0428	1.9048	0.0505	0.0524	3.7624	0.0402	0.0395	1.7413
Average lean-MEA/rich-MEA, (mol CO_2/mol MEA)	0.0512	0.0512	0.0000	0.0405	0.0409	0.9877	0.0490	0.0503	2.6531	0.0379	0.0375	1.0554
CO_2 capture level (%)	98.2	93.79	4.4908	84.2	94.21	11.8883	97.5	94.49	3.0872	91.2	93.20	2.1930
CO_2 penetration (%)	1.8	6.21		15.8	5.79		2.5	5.51		8.8	6.80	
Variable	Case 4											
	Run 5			Run 6			Run 7			Run 8		
	Expt.	Model	Relative error (%)	Expt.	Model	Relative error (%)	Expt.	Model	Relative error (%)	Expt.	Model	Relative error (%)
CO_2 loading of lean-MEA, (mol CO_2/mol MEA)	0.0582	0.0582		0.0443	0.0443		0.0523	0.0523		0.0407	0.0407	
CO_2 loading of rich-MEA, (mol CO_2/mol MEA)	0.0635	0.0645	1.5748	0.0495	0.0516	4.2424	0.0586	0.0598	2.0478	0.0477	0.0481	0.8386
Average lean-MEA/rich-MEA, (mol CO_2/mol MEA)	0.0609	0.0613	0.6568	0.0469	0.0480	2.3454	0.0555	0.0561	1.0695	0.0442	0.0444	0.4525
CO_2 capture level (%)	98.0	90.82	7.3265	84.3	89.36	6.0024	98.1	91.78	6.4424	91	89.84	1.2747
CO_2 penetration (%)	2.0	9.18		15.7	10.64		1.9	8.22		9	10.16	

Table 5
Process conditions for MEA concentration studies.

Variable	20.9 °C lean temperature			39.5 °C lean temperature		
	Run 1	Run 2	Run 3	Run 1	Run 2	Run 3
Rotor speed (RPM)	1000	1000	1000	1000	1000	1000
Lean pressure (atm.)	1	1	1	1	1	1
Flue gas flow rate (kmol/h)	2.87	2.87	2.87	2.87	2.87	2.87
CO_2 composition in flue gas (vol%)	4.35	4.35	4.35	4.35	4.35	4.35
Lean-MEA flow rate (kg/s)	0.66	0.66	0.66	0.66	0.66	0.66
Lean-MEA composition (wt%)						
H_2O	41.39	33.22	22.96	41.39	33.22	22.96
CO_2	3.61	0.178	2.04	3.61	0.178	2.04
MEA	55.00	65.00	75.00	55.00	65.00	75.00

with increase in rotor speed than at 39.5 °C lean MEA temperature even though actual capture level is higher at 39.5 °C lean MEA temperature. The capture level at 39.5 °C lean MEA temperature is close to 100% and as such increasing rotor speed has less effect on it. Again, comparing Figs. 4 and 5 for 20.9 °C lean MEA temperatures in Fig. 4 the capture level increases from 81.61% to 84.93% as rotor speed increases, but in Fig. 5, capture level increase from 83.06% to 90.40% which is more significant than in Fig. 4. The reason for this behaviour is that CO_2 capture level is higher at 75 wt% MEA concentration than at 56 wt% MEA concentration since reaction rate is a function of concentration.

4.2. Effect of MEA concentration on CO_2 capture level

4.2.1. Justification for case study

Increased lean MEA concentration leads to higher capture level and greater tendency for equipment corrosion. Good understanding of this relationship is needed to determine the needed concentration that gives best capture level with less consequence on corrosion.

4.2.2. Setup of the case study

To implement this case study, 1000 rpm rotor speed and 0.66 kg/s lean-MEA flow rate were used. The operating conditions are as shown in Table 5. MEA concentration was varied from 55 wt%, 65 wt% to 75 wt% at two lean MEA temperature conditions, 39.5 °C and 20.9 °C.

4.2.3. Results and discussion

Fig. 6 shows the effect of MEA concentration on CO_2 capture level at the input conditions shown in Table 5. Capture level increases with increase in MEA concentration at 39.5 °C and also at 20.9 °C lean-MEA temperature. The behaviour reflects increase in hydroxide ions per unit volume resulting in higher degree of CO_2 absorption in the lean solvent. This agrees with the findings of Freguia and Rochelle (2003) which showed that the rate coefficient of pseudo-first-order reaction is a function of MEA concentration, meaning that higher concentration of MEA contributes to higher reaction rate. At different temperatures, CO_2 capture level shows similar behaviour with MEA concentration though actual capture level is higher at 39.5 °C lean-MEA temperature than at 20.9 °C lean-MEA temperature. Effect of lean-MEA temperature will be discussed further in Section 4.3.

4.3. Effect of Lean-MEA temperature on CO_2 capture level

4.3.1. Justification for case study

The study is performed to investigate the effect of lean MEA temperature on the performance of RPB absorber. The key driving forces for absorption, mass transfer and chemical reaction, are known to respectively decrease and increase with temperature (Kvamsdal et al., 2010). Conventional absorber performance is already known to be hindered by increase in lean MEA temperature due to the possibility of temperature bulge within the absorber column (Freguia and Rochelle, 2003). Based on this, capture performance with lean MEA temperature should be studied for RPB absorbers.

4.3.2. Setup of the case study

To implement the case study, 1000 rpm rotor speed, 0.66 kg/s lean MEA flow rate. Process conditions are shown in Table 6. The lean MEA temperature is varied from 25 °C, 30 °C, 35 °C, 40 °C, . . ., to 80 °C at 55 wt% and 75 wt% lean MEA concentrations.

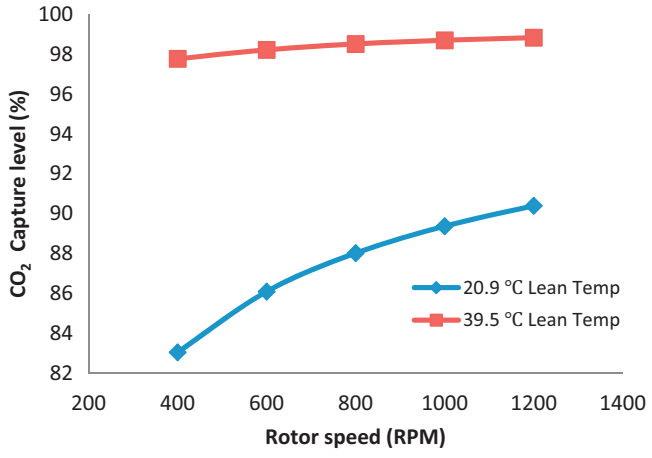

Fig. 5. Effect of rotor speed on CO_2 capture level at 75 wt% MEA.

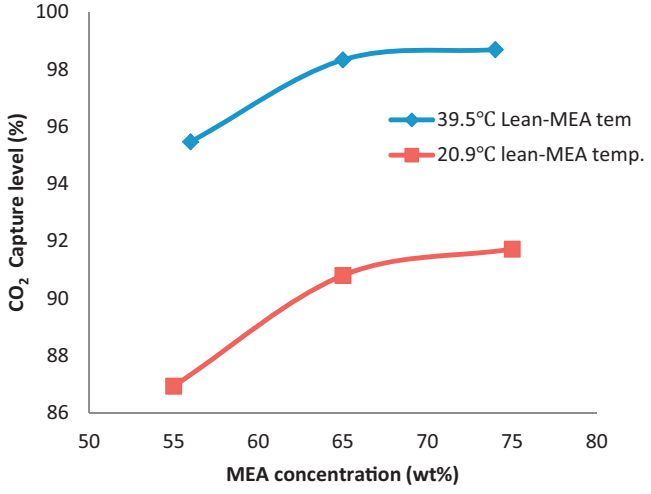

Fig. 6. Effect of MEA concentrations on CO_2 capture level.

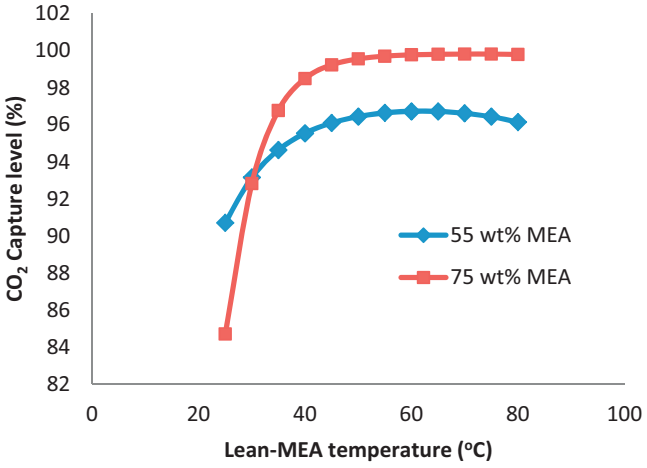

Fig. 7. Effect of lean-MEA temperature on CO_2 capture level.

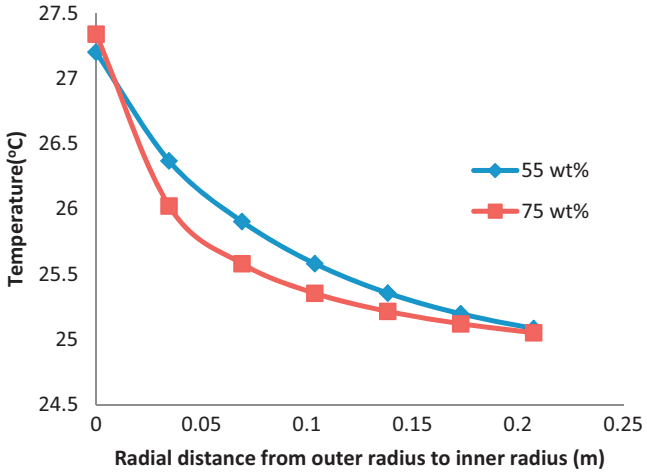

Fig. 8. Liquid temperature profile in RPB absorber at 25 °C lean MEA temperature.

4.3.3. Results and discussions

Fig. 7 shows the effect of varying lean MEA temperature on CO_2 capture level at different lean MEA concentrations (55 wt% MEA and 75 wt% MEA). The results show that CO_2 capture level increases significantly from 25 °C to 50 °C lean MEA temperatures. Lean MEA temperature increase above 50 °C has no significant impact on the CO_2 capture level. Improvement of RPB performance as temperature increases can be associated to decrease in viscosity of the lean MEA solvent as explain by Lewis and Whitman (1924) that the ratio of viscosity to density (kinematic viscosity) of the film fluid is probably the controlling factor in determining film thickness. Haslam et al. (1924) said that if film resistance is directly proportional to film thickness, then film conductivity is the inverse of kinematic viscosity. The effect of temperature on density of gas is great, but temperature affects the density of lean MEA only slightly (Maceiras et al., 2008). Again an increase in temperature causes an increase in viscosity of a gas but the same increase in temperature might greatly lower the viscosity of lean MEA. This improves mass transfer due to thinner liquid film since absorption of CO_2 into alkanolamines solutions is a liquid film controlled process (Jassim et al., 2007). Also Increasing lean solvent temperature leads to increase in chemical reaction rate.

4.4. Temperature profile in RPB absorber

4.4.1. Justification for case study

Temperature bulge in conventional absorber was reported by Freguia and Rochelle (2003), Kvamsdal and Rochelle (2008), Kvamsdal et al. (2009). It limits the overall performance of the absorber. It is necessary to investigate temperature profile in RPB absorbers to determine if it has similar problem.

Table 6
Process conditions for lean MEA temperature studies.

Variable	55 wt% MEA Con.	75 wt% MEA Con.
Rotor speed (RPM)	1000	1000
Lean pressure (atm.)	1	1
Flue gas flow rate (kmol/h)	2.87	2.87
Flue gas composition (vol%)		
H_2O	17.1	17.1
CO_2	4.4	4.4
N_2	78.5	78.5
Lean-MEA flow rate (kg/s)	0.66	0.66
Lean-MEA composition (wt%)		
H_2O	41.03	22.32
CO_2	3.97	2.68
MEA	55.00	75.00

4.4.2. Setup of the case study

To implement this case study, lean MEA flow rate of 0.66 kg/s, rotor speed of 1000 rpm were selected. For 56 wt% lean MEA concentration process conditions refer to Case 1 Run 1 of Table 1 and for 75 wt% lean MEA concentration refer to Case 3 Run 1 of Table 2, in both input conditions the rotor speed is replaced with 1000 rpm. The flue gas temperature was maintained at 47 °C during the study. The temperature profile study was done over two lean MEA temperatures of 25 °C and 50 °C.

4.4.3. Results and discussion

As stated in Kvamsdal and Rochelle (2008) that magnitude and location of temperature bulge are given in term of liquid temperature profile, this is because gas and liquid temperature profiles are similar in shape but the gas temperature profile will be lagged due to the difference in heat capacities of the two phases and the L/G ratio.

Figs. 8 and 9 shows liquid temperature profile in RPB, outer radius where flue gas enters RPB is taken as 0 m. At 55 wt% MEA concentration, temperature profile has a steady gradient for the two temperatures under study. On the other hand, steeper gradient is noticed close to the outer radius. Both results show there is no

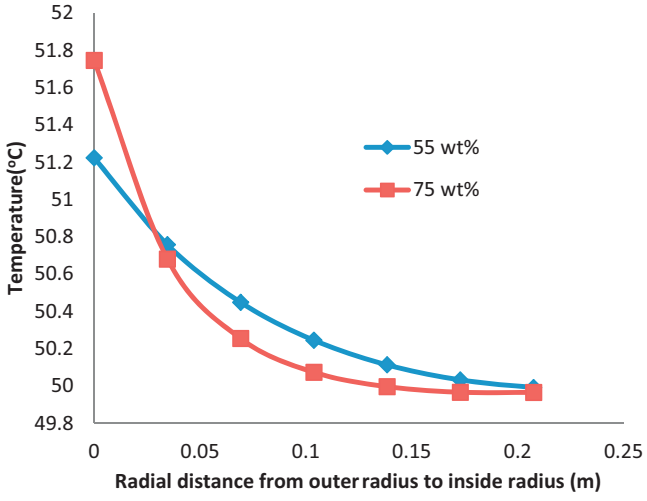

Fig. 9. Liquid temperature profile in RPB absorber at 50 °C lean MEA temperature.

Table 7
Process conditions for conventional and RPB absorbers.

Description	Conventional absorber		RPB absorber	
	Flue gas	Lean-MEA	Flue gas	Lean-MEA
Temperature (K)	323.15	313.25	323.15	313.25
Pressure (10^5 Pa)	1.186	1.013	1.186	1.013
Total flow (kg/s)	0.0228	0.0454	0.0228	0.0440
L/G ratio (kg/kg)	1.99		1.93	
Mass-fraction				
H_2O	0.0030	0.6334	0.0030	0.23426
CO_2	0.0666	0.0618	0.0666	0.02574
N_2	0.9304	0	0.9304	0
MEA	0	0.3048	0	0.74000

temperature bulge in RPB. This is likely due to higher solvent to gas ratio (L/G) which is 30 kg/kg. Kvamsdal and Rochelle (2008) stated for conventional absorber in case where no temperature bulge, the enthalpy of reaction must leave with the gas and liquid. At high liquid rates, the enthalpy will leave with the liquid, while at high gas rates it will leave with the gas. In Figs. 8 and 9 it can be observed that the temperature of lean MEA increases from the inner diameter to the outer diameter. This is because of the gain in the enthalpy of reaction since we have greater liquid rate than the gas rate. Also it can be observed in Figs. 8 and 9 that exit temperature for the solvent at 0 m is higher for 75 wt% MEA concentration than for 55 wt% this is because of greater enthalpy of reaction at higher concentration.

Another factor that contributes to having no temperature bulge in RPB absorber is high mixing capability, which enhances heat transfer and significantly reduces residence time. This is also because there are no liquid build-up since high gravity in RPB stimulates droplet flow and little film flow (Burn's et al., 2000).

From the above findings we can see that RPB absorber does not need inter-cooling provided it is operated at the conditions being studied. From this, we can see that the cost of energy for inter-cooling is saved if we are using RPB absorber. The temperature profile shows that a better column performance could be found in intensified absorber using RPB.

4.5. Comparison between intensified absorber and conventional absorber

4.5.1. Justification for case study

For comparison between the conventional absorber using packed column and the intensified absorber using RPB, detailed study of some of their process parameters is necessary. This section was added to provide a comparison under some fixed conditions such as CO_2 capture level, flue gas flow rate, pressure, temperature and compositions.

4.5.2. Setup of the case study

For this study, Table 7 is used as the input conditions for the conventional absorber and intensified absorber using RPB. In both simulation runs, the capture level was fixed at 90%. The flue gas conditions for the intensified absorber using RPB were also maintained the same for the conventional absorber simulation. L/G ratio used for the conventional absorber was adapted from Canepa et al. (2013). MEA concentration of the conventional absorber was kept at 30.48 wt% to minimize the problem of corrosion. It is believed that size of conventional absorber with packed column as reported by Lawal et al. (2012) is huge and using stainless steel as material of construction is too expensive. But for RPB absorber, the size of the intensified absorber can drastically reduced compared to conventional absorber (Ramshaw and Mallinson, 1981). The use of stainless steel as material of construction is feasible. In the RPB absorber simulation, MEA concentration of 74 wt% is used.

Table 8
Comparison between conventional and RPB absorber.

Description	Conventional absorber	RPB absorber
Height of packing (m)	3.85	0.2885 (r_o) 0.078 (r_i)
Diameter (m)	0.395	0.0377 axial depth
Packing volume (m^3)	0.4718	0.0091
Packing volume reduction		52 times
Volume of unit (m^3)	0.4718[a]	0.04095[b]
Volume reduction factor		12 times
Specific area (m^2/m^3)	145	2132
Void fraction	0.79	0.76
Lean-MEA loading (mol CO_2/mol MEA)	0.2814	0.0483
Rich-MEA loading (mol CO_2/mol MEA)	0.4189	0.1069

[a] Excluding sump.
[b] Using the assumption given by Agarwal et al. (2010).

Modelling and simulation of intensified absorber using RPB was done at rotor speed of 1000 rpm.

4.5.3. Results and discussion

Keeping the CO_2 capture level at 90%, the simulation results of the conventional absorber using packed column and intensified absorber using RPB are shown in Table 8. Calculating the volume of the conventional absorber and RPB absorber without the sump, it was found that conventional absorber is 12 times the volume of RPB using the assumption in Agarwal et al. (2010) that the casing volume of RPB is taken as 4.5 times the RPB volume. In RPB absorber, MEA concentration is higher than what was used in the conventional absorber that is why the lean loading in RPB is lower than what was found in conventional absorber. But looking at the rich loading in both cases it can be seen that there is significant increase in rich-MEA loading in RPB absorber than the convention absorber which means more CO_2 in flue gas stream has been absorbed.

5. Conclusions

This paper presents modelling, validation and analysis of a post-combustion CO_2 capture with MEA in an intensified absorber using RPB. The RPB absorber was modelled in Aspen Plus®. However, some build-in correlations in Aspen Plus® rate-based model were replaced with new correlations suitable for RPB. Rate-based model approach was used and chemical reactions are assumed to be at equilibrium. The model presented in this paper is equivalent to developing a new model for RPB case even though it is still in Aspen Plus®.

Validation of the intensified absorber model was successfully carried out and model predictions showed good agreement with the experimental results. Process analysis was performed to explore the effect of rotational speed, lean-MEA temperature and lean-MEA concentration on CO_2 capture level. It was found that as the lean-MEA temperature increases, the CO_2 capture level increases and as the lean-MEA concentration increases, the CO_2 capture level also increases. Again, as the rotational speed increases, the CO_2 capture level increases due to enhanced mass transfer. Temperature profile study was done for 55 wt% and 75 wt% MEA concentration at lean MEA temperature of 25 °C and 50 °C. The results indicate that temperature bulge is not noticed. The result also shows mass transfer is improved with the use of RPB, also since the RPB absorber is operated at higher temperature, reaction rate is also enhanced. Because there is no temperature bulge in RPB absorber, costs associated with inter-cooling is saved. Comparison between the conventional absorber using packed column and intensified absorber using RPB indicates that the latter gives 12 times reduction in volume without sumps.

Acknowledgement

The authors would like to acknowledge financial support from UK Research Councils' Energy Programme (Ref: NE/H013865/2).

References

Agarwal, L., Pavani, V., Rao, D.P., Kaistha, N., 2010. Process intensification in HIGEE absorption and distillation: design procedure and application. Industrial & Engineering Chemistry Research 49 (20), 10046–10058.

AspenTech, 2010. Aspen Physical Properties System – Physical Property Methods, Available at: http://support.aspentech.com/ (accessed 08.05.12.).

BERR, 2006. Advanced power plant using high efficiency boiler/turbine. Report BPB010. BERR, Department for Business Enterprise and Regulatory Reform, Available at: www.berr.gov.uk/files/file30703.pdf (accessed 06.04.12.).

Biliyok, C., Lawal, A., Wang, M., Seibert, F., 2012. Dynamic modelling, validation and analysis of post-combustion chemical absorption CO_2 capture plant. International Journal of Greenhouse Gas Control 9, 428–445.

Burns, J.R., Jamil, J.N., Ramshaw, C., 2000. Process intensification: operating characteristics of rotating packed beds – determination of liquid hold-up for a high-voidage structured packing. Chemical Engineering Science 55 (13), 2401–2415.

Canepa, R., Wang, M., Biliyok, C., Satta, A., 2013. Thermodynamic analysis of combined cycle gas turbine power plant with post-combustion CO_2 capture and exhaust gas recirculation. Journal of Process Mechanical Engineering 227 (2), 89–105.

Cheng, H., Tan, C., 2011. Removal of CO_2 from indoor air by alkanolamine in a rotating packed bed. Separation and Purification Technology 82 (0), 156–166.

Department of Energy and Climate Change (DECC), 2012. Solid Fuels and Derived Gases Statistics: Data Sources and Methodologies, Available at: http://www.decc.gov.uk/en/content/cms/statistics/energy_stats/source/coal/coal.aspx (accessed 06.05.13.).

Dugas, E.R., (M.S.E. thesis) 2006. Pilot Plant Study of Carbon Dioxide Capture by Aqueous Monoethanolamine. University of Texas, Austin, USA.

Freguia, S., Rochelle, G.T., 2003. Modeling of CO_2 capture by aqueous monoethanolamine. AIChE Journal 49 (7), 1676–1686.

Haslam, R.T., Hershey, R.L., Keen, R.H., 1924. Effect of gas velocity and temperature on rate of absorption. Industrial and Engineering Chemistry 16 (12), 1224–1230.

Jassim, M.S., (Ph.D. thesis) 2002. Process Intensification: Absorption and Desorption of Carbon Dioxide From Monoethanolamine Solutions Using HIGEE Technology. University of Newcastle upon Tyne, UK.

Jassim, M.S., Rochelle, G., Eimer, D., Ramshaw, C., 2007. Carbon dioxide absorption and desorption in aqueous monoethanolamine solutions in a rotating packed bed. Industrial & Engineering Chemistry Research 46 (9), 2823–2833.

Kvamsdal, H.M., Rochelle, G.T., 2008. Effects of the temperature bulge in CO_2 absorption from flue gas by aqueous monoethanolamine. Industrial & Engineering Chemistry Research 47 (3), 867–875.

Kvamsdal, H.M., Jakobsen, J.P., Hoff, K.A., 2009. Dynamic modeling and simulation of a CO_2 absorber column for post-combustion CO_2 capture. Chemical Engineering and Processing: Process Intensification 48 (1), 135–144.

Kvamsdal, H.M., Hetland, J., Haugen, G., Svendsen, H.F., Major, F., Kårstad, V., Tjellander, G., 2010. Maintaining a neutral water balance in a 450 MWe NGCC-CCS power system with post-combustion carbon dioxide capture aimed at offshore operation. International Journal of Greenhouse Gas Control 4 (4), 613–622.

Lawal, A., Wang, M., Stephenson, P., Yeung, H., 2009a. Dynamic modelling of CO_2 absorption for post combustion capture in coal-fired power plants. Fuel 88 (12), 2455–2462.

Lawal, A., Wang, M., Stephenson, P., Yeung, H., 2009b. Dynamic modeling and simulation of CO_2 chemical absorption process for coal-fired power plants. Computer Aided Chemical Engineering 27, 1725–1730.

Lawal, A., Wang, M., Stephenson, P., Koumpouras, G., Yeung, H., 2010. Dynamic modelling and analysis of post-combustion CO_2 chemical absorption process for coal-fired power plants. Fuel 89 (10), 2791–2801.

Lawal, A., Wang, M., Stephenson, P., Obi, O., 2012. Demonstrating full-scale post-combustion CO_2 capture for coal-fired power plants through dynamic modelling and simulation. Fuel 101, 115–128.

Lewis, W.K., Whitman, W.G., 1924. Principles of gas absorption. Industrial and Engineering Chemistry 16 (12), 1215–1220.

Llerena-Chavez, H., Larachi, F., 2009. Analysis of flow in rotating packed beds via CFD simulations – dry pressure drop and gas flow maldistribution. Chemical Engineering Science 64, 2113–2126.

MacDowell, N., Florin, N., Buchard, A., Hallett, J., Galindo, A., Jackson, G., Adjiman, C.S., Williams, C.K., Shah, N., Fennell, P., 2010. An overview of CO_2 capture technologies. Energy and Environmental Science 3 (11), 1645–1669.

Maceiras, R., Álvarez, E., Cancela, M.Á., 2008. Effect of temperature on carbon dioxide absorption in monoethanolamine solutions. Chemical Engineering Journal 138 (1–3), 295–300.

Onda, K., Sada, E., Takeuchi, H., 1968. Gas absorption with chemical reaction in packed columns. Journal of Chemical Engineering of Japan 1 (1), 62–66.

Prada, R.J., Martinez, E.L., Maciel, M.R.W., 2012. Computational study of a rotating packed bed distillation column. In: Proceedings of the 22nd European Symposium on Computer Aided Process Engineering, London, 17–20 June 2012.

Ramshaw, C., Mallinson, R.H., 1981. Mass transfer process. US Patent 4283255.

Reay, D., 2008. The role of process intensification in cutting greenhouse gas emissions. Applied Thermal Engineering 28 (16), 2011–2019.

Trevor, K., 1998. Process Plants: A Handbook for Inherently Safer Design. Taylor and Francis Ltd., USA.

Tung, H.H., Mah, R.S.H., 1985. Modeling liquid mass transfer in HIGEE separation process. Chemical Engineering Communications 39 (1–6), 147–153.

Wang, M., Lawal, A., Stephenson, P., Sidders, J., Ramshaw, C., 2011. Post-combustion CO_2 capture with chemical absorption: a state-of-the-art review. Chemical Engineering Research and Design 89 (9), 1609–1624.